Received: 6 April 2019 | Revised: 14 January 2020 | Accepted: 11 March 2020

DOI: 10.1111/tbed.13553

ORIGINAL ARTICLE

Transboundary and Emerging Diseases WILEY

A quantitative analysis of the spatial and temporal evolution patterns of the bluetongue virus outbreak in the island of Lesvos, Greece, in 2014

Chrisovalantis Malesios[1,2] | Myrsini Chatzipanagiotou[3] | Nikolaos Demiris[4,5] | Apostolos Kantartzis[6] | Georgios Chatzilazarou[6] | Stauroula Chatzinikolaou[7] | Polychronis Kostoulas[3]

[1]Department of Agricultural Economics and Rural Development, Athens Agricultural University, Athens, Greece

[2]Aston Business School, Aston University, Birmingham, UK

[3]School of Health Sciences, University of Thessaly, Karditsa, Greece

[4]Department of Statistics, Athens University of Economics and Business, Athens, Greece

[5]Cambridge Clinical Trials Unit, University of Cambridge, Cambridge, UK

[6]Department of Forestry and Management of the Environment and Natural Resources, Democritus University of Thrace, Orestiada, Greece

[7]Directorate of Rural Economy and Veterinary Medicine, Regional unit of Lesvos, Mytilene, Greece

Correspondence
Chrisovalantis Malesios, Department of Agricultural Economics and Rural Development, Athens Agricultural University, Athens 118 55, Greece.
Email: malesios@aua.gr

Funding information
Athens University of Economics and Business

Abstract

Bluetongue virus (BTV) causes an infectious disease called bluetongue, a vector-borne viral disease of ruminants, which has major implications and causes severe economic damage due to its effect on livestock. These economic costs are mostly ascribed to the trade restrictions imposed during the epidemic period. In August 2014, an epidemic of bluetongue occurred in the island of Lesvos, Greece. The epidemic was severe and evolved over time, lasting until December 2014. The total cases of infected farms were 490, including a total number of 136,368 small ruminants. In this paper, we describe a bluetongue virus serotype 4 (BTV-4) epidemic and utilize Bayesian epidemic models to capture the spatio-temporal spread of the disease. Our study provides important insights into the drivers of BTV transmission and has implications for designing control strategies. The results showed strong spatial autocorrelations, with BTV being more likely to spread between farms located nearby. The spatial modelling results proposed a certain spatial radius (~12 km) around the onset of a similar epidemic for imposing restrictions on animal movement, which can be sufficient for the control of the disease and limit economic damage.

KEYWORDS

Bayesian model, bluetongue virus, Greece, Lesvos, spatio-temporal evolution

1 | INTRODUCTION

Bluetongue (BT) is an infectious, vector-borne disease of ruminants caused by the bluetongue virus (BTV), a member of the genus *Orbivirus* which belongs to the family Reoviridae. Twenty-seven serotypes of BTV have so far been isolated and identified (Rojas, Rodríguez-Martín, Martín, & Sevilla, 2019). BTV is transmitted between hosts by bites of *Culicoides* midges and replicates in all ruminants, but severe disease is restricted mainly to certain breeds of sheep and some deer (Taylor, 1986).

BT can be enzootic in areas where the mammalian reservoirs, the virus and the insect vectors have the opportunity to coexist in

climatic conditions conducive to BTV replication and transmission (Caporale et al., 2014). As a result, BTV was historically present exclusively in tropical and subtropical areas of the world, where suitable conditions exist. However, over the last decades, the global distribution of BT has expanded dramatically, potentially due to a variety of factors, including an increased global travel and commerce, deforestation and recent global climatic changes in combination with the related spread of the main BTV vectors of *Culicoides imicola* (Caporale et al., 2014; Purse et al., 2005; Randolph & Rogers, 2010) and *Obsoletus* complex (Federici et al., 2019). In addition, recent evidence from California indicated the possibility that the virus can survive through the winter in long-living *C. soronensis* female midges, which had been infected during the previous flying activity period (Mayo et al., 2014). The latter can be affected by temperature, light intensity, lunar cycles, relative humidity, wind velocity and other weather conditions, with the mean distance flown by female *Culicoides* spp. being about 2 km (Mellor, 1990).

In Europe, BT occurred for the first time between 1956 and 1960 in Spain and Portugal (Manso-Ribeiro et al., 1957), while the first epidemic of the disease in Greece occurred on the island of Lesvos in October 1979 and was caused by serotype 4 (Nomikou, Mangana-Vougiouka, & Panagiotatos, 2004). After 1998, BT spread from Turkey to the Greek mainland and northwards and, by 2001, reached Italy (Calistri et al., 2004; Nomikou et al., 2004). Between 2006 and 2008, an extensive epidemic of BTV-8 occurred in Europe (Wilson & Mellor, 2009). At the end of May 2014, a case of bluetongue virus serotype 4 was clinically diagnosed in Greece, in south Peloponnese, and by the end of August 2014, it was prevalent in the whole country, including the island of Lesvos (World Organisation for Animal Health, 2015). Cases of the disease caused by BTV-4 were then (July–December 2014) reported in Albania, Croatia, the Republic of Northern Macedonia, Hungary, Montenegro, Romania, Bulgaria, Serbia and Turkey (Niedbalski, 2015; World Organisation for Animal Health, 2015).

Notwithstanding suggestions that vaccinations could have led to limit the disease at the initial stages in Greece (Vasileiou et al., 2016), the authorities had opted to limit the epidemic by controlling insect vector activity, vector surveillance, restriction of animal movement, clinical examinations followed by blood sampling and testing in small ruminants with clinical suspicion and in sentinel bovine as part of surveillance. In May 2015, vaccinations of animals had been authorized and two vaccines had been licensed for use in ruminants in Greece (Greek Ministry of Rural Development and Food, 2015; Kyriakis et al., 2015). Vaccinations started immediately thereafter and no cases of the disease had been reported by the Greek authorities until the end of June 2015 (World Organisation for Animal Health, 2014). In 2017, a BTV outbreak was reported on the Greek islands of Samos and Kos, and in 2018 on the islands of Ikaria and Rhodes (Greek Ministry of Rural Development and Food, 2019). Until October 2018, no BTV cases have been reported in the island of Lesvos. However, in January 2019, a few days before the end of the disease control programme conclusion including the end of quarantine, one case of BTV-16 was confirmed in cattle, in the area of Petra, as announced by the Directorate of Rural Economy and Veterinary Medicine, regional unit of Lesvos (DREVM). The legal definition of a BT case was described as follows: (a) when a ruminant exhibits clinical signs compatible with BT, (b) when a sentinel bovine animal presents seroconversion, (c) when an animal is serologically BTV-positive or BTV has been detected by molecular techniques and (d) when BTV is isolated from an identified animal (Greek Ministry of Rural Development and Food, 2015).

In the current paper, the authors provide descriptive summaries of the spatial and temporal patterns of the available data regarding the 2014 epidemic in Lesvos Island, Greece. Measures of spatial autocorrelation in order to explore potential spatial patterns in disease transmission are also presented. Additionally, in the present study, a spatio-temporal regression-based Bayesian modelling approach is developed in order to characterize the spread of the BT virus between the infected farms of the island. The transmission was modelled via a spatial kernel-based component describing the spread of disease from infected to non-infected farms. Our model includes an Ornstein–Uhlenbeck (OU) process, a continuous-time model used for absorbing model mis-specification, capturing distributional deviations and the inherent serial correlation of the data.

2 | MATERIALS AND METHODS

2.1 | Data

2.1.1 | Study area

The study area was the Greek island of Lesvos, located in the Northeastern Aegean Sea. It has an area of 1,633 km^2 with 320 km of coastline, making it the third largest island in Greece. It is close to Turkey, separated by a narrow Strait (see Figure 1). A total of 165,831 small ruminants had been reported by the DREVM as susceptible, farmed within 617 holdings, while the reported number of bovine was 6,696 animals. In previous years, serotypes BTV-1, BTV-4, BTV-9 and BTV-16 were present in the island (Kyriakis et al., 2015; Nomikou et al., 2004). On 17 December 2013, the average temperature in Lesvos was 8°C, with 66% humidity and 13 km/hr wind speed as recorded by Mytilene Airport Weather Station, while on 30 May 2014, the average temperature was 21°C, with 68% humidity and 8 km/hr wind speed.

2.1.2 | Data collection

Collected data include the location—in the form of geographical coordinates—for each BTV-infected holding and were acquired by the DREVM. WGS 84 is the reference coordinate system used by the Global Positioning System and is the one used in our study for defining the coordinates. In the present analysis, a farm was considered as infected if at least one animal of the farm was detected with BTV. Diagnosis was based on the laboratory confirmation of BTV-positive blood samples following the immediate clinical examination

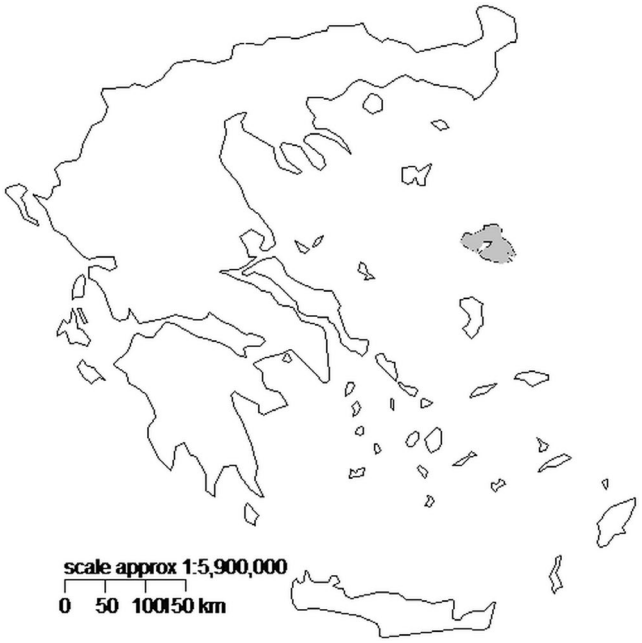

FIGURE 1 Island of Lesvos, Greece (in grey colour)

upon suspicion of the disease by an official veterinarian. Laboratory techniques used to confirm a BT case included competitive-ELISA and real-time RT-PCR (World Organisation for Animal Health, 2013). Temporal information such as time of infection, which is important for identifying the temporal progress of disease, was also made available. The date of blood sampling on clinical suspicion in each farm was acquired by the DREVM. There were only few cases of clinical suspicion which were not laboratory confirmed.

In addition, aggregate farm-level data on the number of sheep and goat flocks for each municipality of the island were recorded and utilized for subsequent analyses, especially concerning the spatial epidemic modelling. We assumed in the subsequent analyses that the unit of population is the farm. The aggregated information on the number of susceptible farms in the island for each municipality provided by the DREVM did not contain the exact spatial location for each farm. Therefore, each farm was randomly allocated in space within each municipality using the Random Points tool available in the QGIS software (QGIS Development Team, 2015). In particular, using the command 'Randomly generate points within the polygon', we placed randomly distributed points within the boundaries of the polygons (in this case the boundaries of each municipality in the island). Next, having predefined the sampling of random point locations based on characteristics such as the frequency, that is the field with the number of points of each polygon and the minimum distance allowed, we have sampled the random spatial distribution of the farms within each municipality.

2.2 | Purely spatial measures

We examined the characteristics of the temporal and spatial spread of BT during the 2014 epidemic, by using appropriate spatial measures. Specifically, we estimated the Global Moran's *I* and the Geary's *C* statistic in order to test for spatial autocorrelation in disease transmission (Lessler, Salje, Grabowski, & Cummings, 2016). We later employ suitable Bayesian spatio-temporal models that utilize both spatial and temporal information as well as including a continuous-time stochastic Ornstein–Uhlenbeck part that allows modelling the inherent serial correlation of the data-generating mechanism (Malesios, Demiris, Kalogeropoulos, & Ntzoufras, 2017; Oravecz & Tuerlinckx, 2011).

2.2.1 | Global Moran's *I*

The global Moran's *I* test (Li, Calder, & Cressie, 2007; Moran, 1950) is a measure of spatial autocorrelation used to test for spatial clustering of a region throughout the study area without the ability of locating specific clusters sites. The global weight matrix is used to define the spatial relationships so that regions close in space are given a greater weight. Moran's *I* takes values between −1 and +1 with positive values (near +1) indicating the presence of clustering while a negative *I* value indicates tendency towards dispersion. For the Global *I* statistic, the null hypothesis states that the attribute being analysed is randomly distributed among the features in the selected study area. The *I* test statistic is defined as:

$$I = \frac{n}{S_0} \frac{\sum_i \sum_j w_{ij} (x_i - \bar{x}) (x_j - \bar{x})}{\sum_i (x_i - \bar{x})^2}, \quad (1)$$

where n is the number of observations on a variable x at locations i, j, $\bar{x}$ is the mean of the x variable, w_{ij} are the elements of the weight matrix, and S_0 is the sum of the elements of the weight matrix: $S_0 = \sum_i \sum_j w_{ij}$.

In order to identify the location of potentially significant clusters, suitable heat maps are also presented. All spatio-temporal maps for the visualization of the spread of the epidemic were constructed with the use of the QGIS software.

2.2.2 | Geary's *C*

Geary's *C* statistic (Geary, 1954) is based on the deviations in responses of each observation with one another and is defined as:

$$C = \frac{n-1}{2S_0} \cdot \frac{\sum_i \sum_j w_{ij} (x_i - x_j)^2}{\sum_i (x_i - \bar{x})^2}, \quad (2)$$

Geary's *C* ranges from 0 (maximal positive autocorrelation) to a positive value for high negative autocorrelation. Note that its expectation is 1 in the absence of autocorrelation and regardless of the specified weight matrix (Sokal & Oden, 1978).

Moran's I is more sensitive to extreme values and is thought of as a global measure, whereas the Geary's C is more sensitive to differences between values in neighbouring areas.

2.3 | Spatio-temporal modelling

To estimate the BTV occurrence at the farm-level, a spatio-temporal disease transmission model was developed following the Bayesian paradigm. The total number of farms is subdivided in two sets, the farms which were infected during the epidemic and the remaining set of ultimately susceptible farms.

2.3.1 | The model

We now describe the general class of spatio-temporal epidemic models utilized for our analysis. If y_i denotes the number of herds infected with BT virus at time t_i where $i \in \{0,1,...,132\}$ is ordered chronologically by day for the complete duration of the epidemic period, then it is assumed that the number of infected herds y_i at time t_i is described by the following model:

$$y_i \sim g\left(y_i|\theta_i\right) \tag{3}$$

$$\theta_i = h\left(\lambda_i\right) = \exp\left(\lambda_i\right) \tag{4}$$

$$d\lambda_t = \phi\left(\lambda_t - \mu_t\right)dt + dB_t \tag{5}$$

where g denotes the assumed distribution of the data and λ_i is the rate at which new infections take place during the disease progress. Equation (5) is used to model the serial correlation in the data, in the form of an Ornstein–Uhlenbeck process (see e.g. Taylor, Cumberland, & Sy, 1994). Here, B_t denotes standard Brownian motion and ϕ the mean reversion parameter (i.e. the rate at which the process returns to its mean) of the OU process. The piecewise constant deterministic process μ_t is given by:

$$\mu_t = \begin{cases} \mu^{(0)} \text{ if } 0 \le t < t_1 \\ \mu^{(1)} \text{ if } t_1 \le t < t_2 \\ \vdots \\ \mu^{(132)} \text{ if } t_{131} \le t < t_{132} \end{cases} \tag{6}$$

with each $\mu^{(i)}$ corresponding to $t_i \le t < t_{i+1}\ i = (0,1,...,132)$ given by:

$$\mu^{(i)} = \beta_0 + \kappa\left(d_i\right). \tag{7}$$

In Equation (7), β_0 represents the intercept and $\kappa\left(d_{k\ell}\right)$ the spatial kernel for the incorporation of spatial information associated with the rate at which infection passes from an infected farm ℓ at times $i-j\,(j=1,2,3,4)$ to a susceptible farm k at time i. We assumed a 4-day incubation period (Scott, 2011; World Organisation for Animal Health, 2013). The kernel component of the model captures the fact that BT is more likely to spread between farms located nearby than farms located more distant apart:

$$\kappa\left(d_i\right) = \begin{cases} \frac{1}{|d_i|}\sum_{k\in S_i}\sum_{\ell\in I_{i-j}} \kappa\left(d_{k\ell}\right) & \text{if at least one } y_{i-j} > 0\ (j=1,2,3,4) \\ \kappa\left(d_{\min}\right) & \text{if all } y_{i-j} = 0\ (j=1,2,3,4) \end{cases} \tag{8}$$

Here, $|d_i|$ denotes the cardinality of d_i, the term $\kappa\left(d_{k\ell}\right)$ denotes some specified function of the distance between the infected and susceptible farms based upon their distance $d_{k\ell}$ and $d_{\min}$, which is fixed a priori, restricts the minimum distance over which infections do not occur (Deardon et al., 2010). For our analysis, we have set $d_{\min} = 70$ km. The functional forms that were tested for κ are given in Table 1, with α being the kernel parameter. Selection of the most appropriate form was based on a variety of relevant functions that have already been utilized in the relevant literature for the modelling of the spatial transmission of BT, namely an Exponential (A), Gaussian (B) and Fat-tailed (C) kernel functions (see Szmaragd et al., 2009).

Regarding the specification of function g in Equation (3), we examined various options such as the Poisson (P) and the negative binomial (NB) distributions. Additionally, in order to account for the presence of excess zeros in disease occurrence, the zero-inflated Poisson (ZIP) and zero-inflated negative binomial (ZINB) model distributions were also considered (for more details see Malesios et al., 2017; Malesios et al., 2016).

We fitted 12 models in total, combining the four distributional specifications (i.e. Poisson, Negative Binomial, ZIP and ZINB) and the three forms of kernel functions (i.e. Exponential (A), Gaussian (B) and Fat-tailed (C)).

2.3.2 | Model selection

We additionally present the results of selecting the most-suited model by evaluating their performance on capturing disease evolution. Deviance-based measures have been utilized for the comparison and selection among the P, NB, ZIP and ZINB models due to the well-known equivalence in model selection using cross-validation or AIC (see Stone, 1977). Smaller values indicate better fit (Spiegelhalter, Best, Carlin, & Linde, 2002).

TABLE 1 The spatial kernels $\kappa\left(d_{k\ell}\right)$ included in the spatio-temporal models

NOTATION	$\kappa\left(d_{k\ell}\right)$	Parameter	Reference
A(exponential)	$\alpha\exp\left(-\alpha d_{k\ell}\right)$	α	Szmaragd et al. (2009)
B(Gaussian)	$\frac{\alpha}{\sqrt{\pi}}\exp\left(-\alpha^2 d_{k\ell}^2\right)$	α	Szmaragd et al. (2009)
C(fat-tailed)	$\frac{\alpha}{4}\exp\left(-\alpha^{1/2} d_{k\ell}^{1/2}\right)$	α	Szmaragd et al. (2009)

2.3.3 | Implementation

A weakly informative $N(0,10^4)$ prior was used for the intercept β_0 and the parameters of the kernel component κ. All models were estimated using the WinBUGS (Lunn, Thomas, Best, & Spiegelhalter, 2000) software. The posterior results were obtained after discarding the initial 5,000 iterations, using an additional sample of 10,000 iterations (using a thinning lag of 10 for minimizing autocorrelation).

3 | RESULTS

3.1 | Descriptive analysis on the 2014 bluetongue epidemic in Lesvos Island, Greece

A total of 490 farms were infected between August and December of 2014 in Lesvos Island, Greece. The total amount of sheep and goats in infected farms was 136,368 (approximately 98% sheep and 2% goats), while no bovine was infected. Figure 2 below displays the weekly temporal distribution of the bluetongue epidemic cases—considering each farm as a single unit.

As we observe from Figure 2, the epidemic peaked during the end of September and first week of October 2014. The epidemic persisted with high number of infected herds until the end of October 2014. For a more detailed description of the temporal progress of the disease, see Table A1 in the Appendix.

The spatial distribution and density of sheep and goat farms in the island of Lesvos in 2014 is shown in Figure 3. The majority of sheep and/or goat farms network lies within the northwest part of the island, mainly in the prefectures of Kaloni and Mantamados.

3.2 | Spatio-temporal description of the epidemic

In Figure 4, the different heat maps represent the spatio-temporal spread of the disease between August and December 2014 in the island. The heat maps are presented in order to visualize the density of disease occurrence over time. Each map includes the individual farm infections for a time period of 15 days, starting from 1 August 2014. A more detailed description of the progress of the disease is depicted in Figure A1 in the Appendix, showing the corresponding

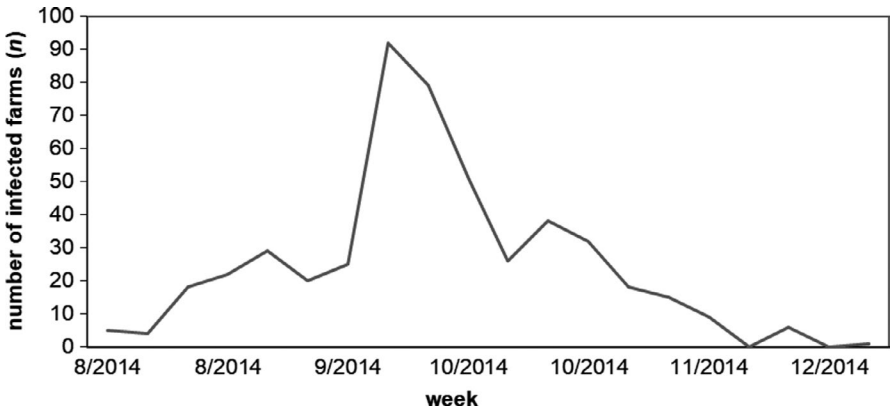

FIGURE 2 Temporal distribution of bluetongue outbreaks in Lesvos, Greece (8/5/2014–12/15/2014)

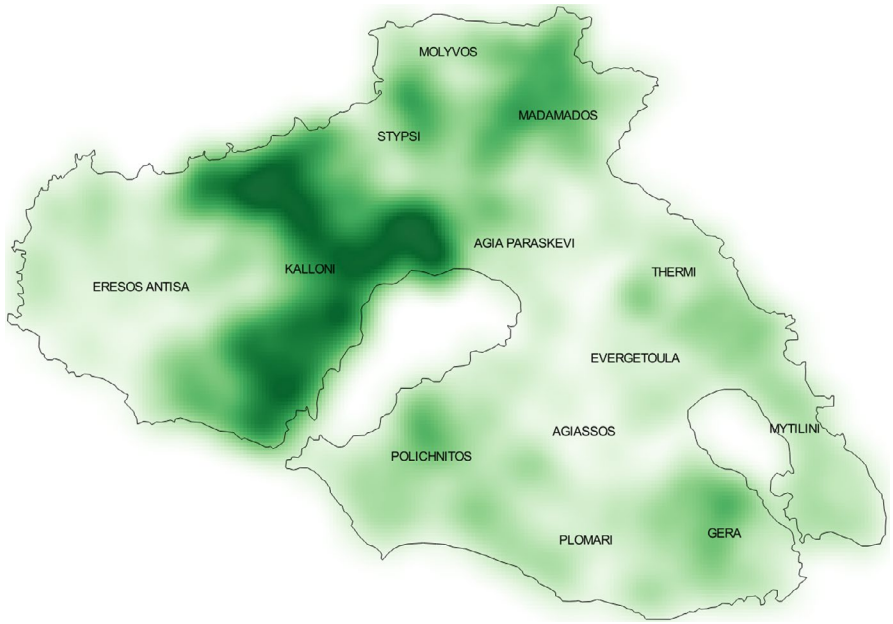

FIGURE 3 Heat map of the spatial distribution of all the sheep and goat farms in Lesvos for the year 2014

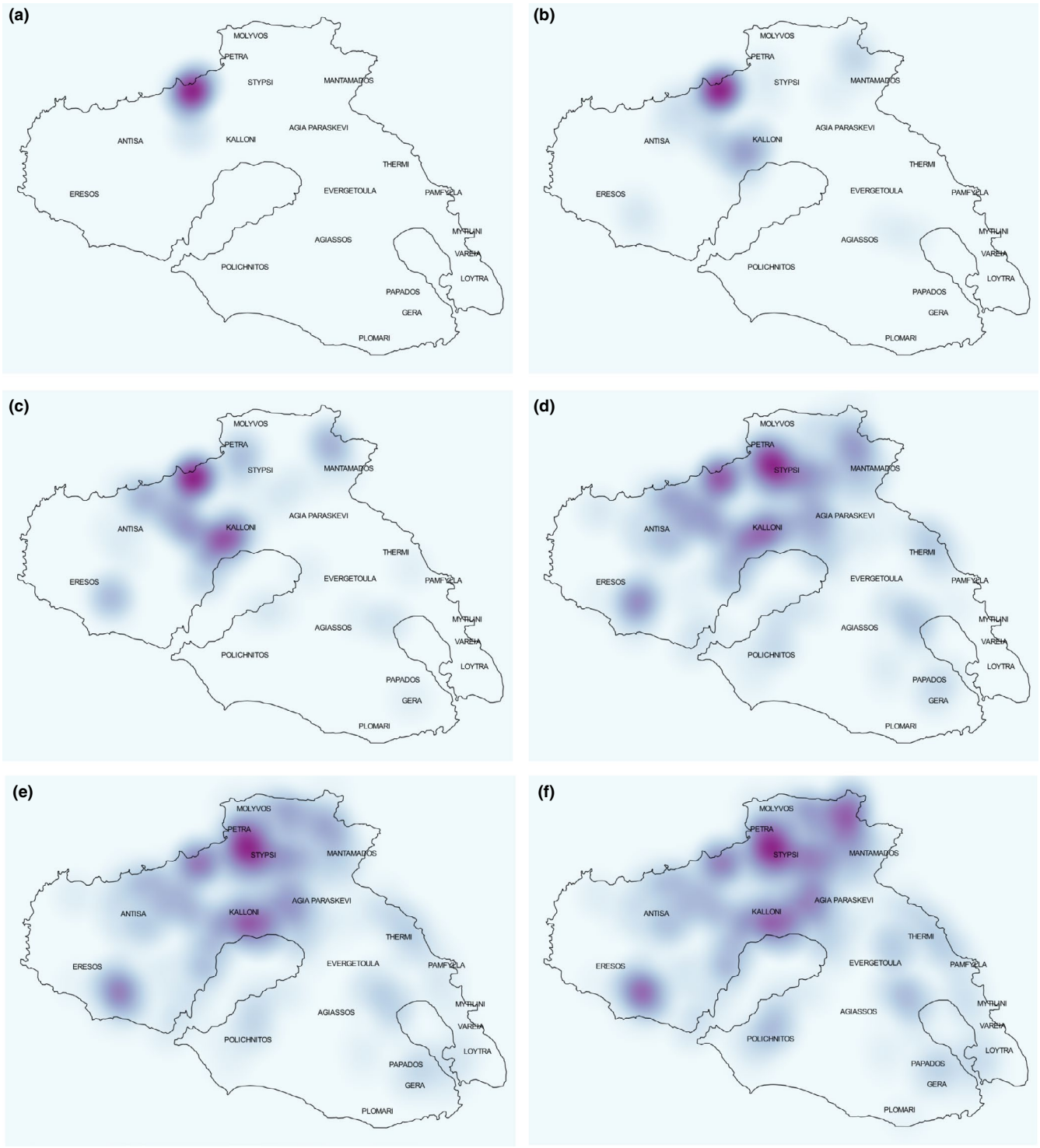

FIGURE 4 Heat maps describing the spatial density of BT disease occurrence in the island of Lesvos during the period August–December 2014

pockets of high BT concentration. The maps suggest that the highest densities of BT disease throughout the progress of the epidemic are located mainly in the northern parts of the island and specifically in the wider regions of Kalloni, Agia Paraskevi, Mantamados, Stypsi and Petra. Another important pocket of high concentration is located in the wider region of Eresos.

The starting point of the epidemic in August of 2014 was located in the northern part of the island, close to the villages of Skoutaros and Filia (see Figure 4; Figure A1, map A). Subsequently, the disease spread further to other parts of northern and eastern part of the island, to Mantamados, Petra and Kalloni regions. The longest transmission was observed in two infected farms located near the

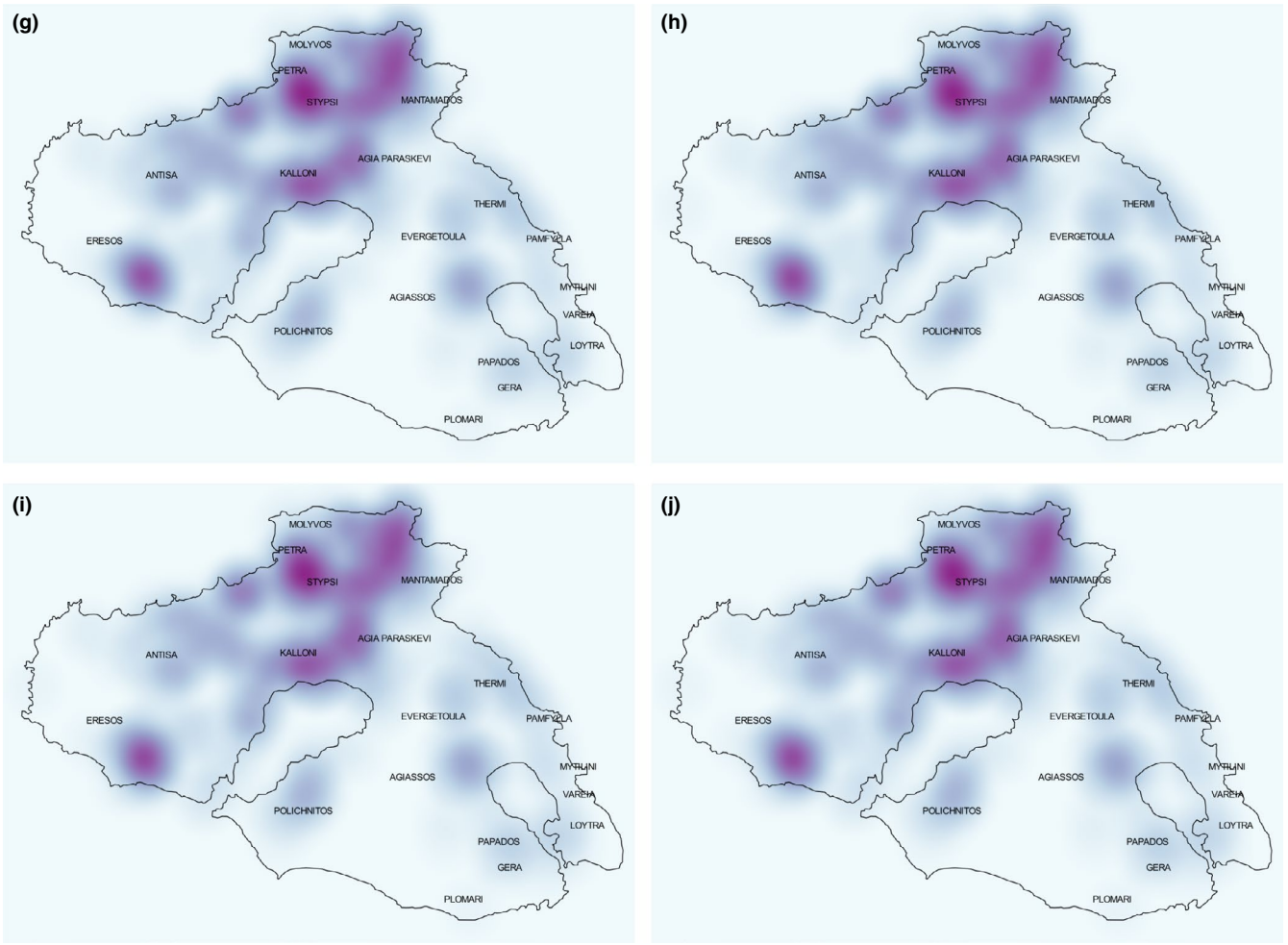

FIGURE 4 (Continued)

Agiassos village in the centre of the island Figure 4; Figure A1, map B). The epidemic continued to affect nearby premises between 9/01/2014 and 9/15/2014, with multiple infections, mostly in the regions of Kalloni, Petra, Mandamados, Antisa, Agia Paraskevi and Eressos Figure 4; Figure A1, map C). The total number of infections during this period of time reached 50 infected premises.

Subsequently, more intense spread of BT virus occurred (a total of 160 infected farms), covering almost every part of the island during the period between 9/15/2014 and 9/30/2014 (Figure 4; Figure A1, map D). During the 10/1/2014 to 10/15/2014 period, new infections occurred in the South-east coastal area of Lesvos. Finally, by 10/29/2014, the disease reached the south edge of Lesvos, with a new infection located near the town of Plomari (Figure 4; Figure A1, map F). During November and December, the incidence of the epidemic gradually declined, with 42 new cases in November (Figure 4; Figure A1, maps G–H) and only seven infections in December (Figure 4; Figure A1, maps I–J). The last case of infection was detected close to the village of Agia Paraskevi on 12/15/2014 (Figure 4; Figure A1, map J).

TABLE 2 Moran's *I* statistic measuring the spatial autocorrelation for the different time periods of the BT epidemic in Lesvos Island, Greece, during 2014

	Moran's *I*	*z* score	*p*-value
8/01/2014–8/14/2014	0.298	1.56	.059*
8/15/2014–8/31/2014	0.105	1.25	n.s.
9/01/2014–9/14/2014	0.111	1.33	n.s.
9/15/2014–9/30/2014	0.144	2.28	.011**
10/01/2014–10/14/2014	0.098	1.96	n.s.
10/15/2014–10/31/2014	0.131	3.07	.002***
11/01/2014–11/14/2014	0.139	3.54	<.001***
11/15/2014–11/30/2014	0.134	3.44	<.001***
12/01/2014–12/14/2014	0.138	3.58	<.001***
12/15/2014–12/31/2014	0.139	3.59	<.001***

Abbreviation: n.s.: non-significant.

***Significant at a 1% level.

**Significant at a 5% level.

*Significant at a 10% level.

Table 2 shows the values derived from the spatial autocorrelation calculations of the Moran's *I* test, for each time period (15 days).

Moran's *I* values revealed that the spatial distribution of the BT cases in the Lesvos Island is spatially non-random. Specifically, the null hypothesis that the BTV cases were randomly distributed was rejected for the majority of the time periods, suggesting spatial autocorrelation for BT incidence in the Lesvos Island (Table 2). However, BTV spread randomly during the first stages of the epidemic, for three time periods, that is between 8/15/2014-8/31/2014, 9/01/2014-9/14/2014 and 10/01/2014-10/14/2014. Additional random spread is observed during the time period between 10/01/2014-10/14/2014, corresponding to the period where the BT disease spread further to regions near the capital city of Mytilene (see Figure 4, map E).

Further, under the null hypothesis of no global spatial autocorrelation, the results of Geary's *C* coefficients indicate a positive spatial autocorrelation in our data (Table 3).

3.3 | Spatio-temporal regression modelling results

Among the 12 candidate models (Table 4), the ZIP class had the best fit to the data in the sense that its posterior mean deviance is the smallest. Further, the best fitted kernel was the Gaussian kernel B with the exponential kernel A being very close. In contrast to the good fit of the two light-tailed kernels, the worst fit was observed for the fat-tailed kernel C across the different distributional assumptions. In summary, these results indicate that BTV is more likely to spread between farms located nearby as opposed to farms more distant apart.

Next, for the best spatio-temporal model (i.e. ZIP model with a Gaussian kernel B), we present the posterior estimates of model parameters (posterior medians and 95% credible intervals) in Table 5. Note that in all the spatio-temporal models, the spatial kernel parameter α was significant, suggesting a positive association between new infections and spatial spread of the disease. For the best model, the distance affects both the occurrence (infection rate part) and non-occurrence of the disease (excess zero part), since the parameter α is statistically significant in both componenets.

TABLE 3 The Geary's *C* statistic for measuring the spatial autocorrelation for the different time periods of the BT epidemic in Lesvos Island, Greece, during 2014

	Geary's *C*	*z* score	*p*-value
8/01/2014–8/14/2014	0.536	1.47	.07*
8/15/2014–8/31/2014	0.105	1.01	n.s.
9/01/2014–9/14/2014	0.362	1.48	n.s.
9/15/2014–9/30/2014	0.571	2.09	.01*
10/01/2014–10/14/2014	0.709	1.77	.07*
10/15/2014–10/31/2014	0.674	2.44	.01*
11/01/2014–11/14/2014	0.657	2.79	.005***
11/15/2014–11/30/2014	0.675	2.68	.007***
12/01/2014–12/14/2014	0.672	2.74	.003***
12/15/2014–12/31/2014	0.672	2.73	.006***

Abbreviation: n.s.: non-significant.

***Significant at a 1% level.

**Significant at a 5% level.

*Significant at a 10% level.

TABLE 5 Posterior medians and corresponding 95% credible intervals of model parameters (ZIP model)

Parameter	Infection rate part	Zero part
Intercept	1.117 (0.448, 1.642)	−0.838 (−1.667, −0.18)
α (kernel parameter)	0.17 (0.022, 0.342)	0.042 (0.022, 0.066)
ϕ(rate of OU process)	0.465 (0.316, 0.517)	—

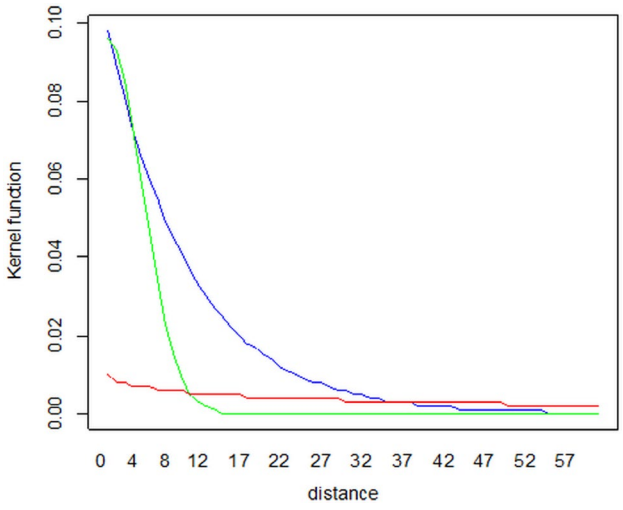

FIGURE 5 Spatial transmission kernel κ as was estimated for the 2014 BT epidemic data (— Kernel A, — Kernel B, — Kernel C)

	Distribution			
Kernel	P	NB	ZIP	ZINB
A (exponential)	393.9 (456.2)	524.5 (531)	272.7 (—)	492.7 (—)
B (Gaussian)	397.9 (458.4)	523.8 (530.5)	**272.5** (—)	522.7 (—)
C (fat-tailed)	405.9 (467.9)	529.8 (534.4)	276.2 (—)	523.4 (—)

TABLE 4 Posterior mean deviance ($\overline{D}$) for the various fitted models (DIC in the parentheses)

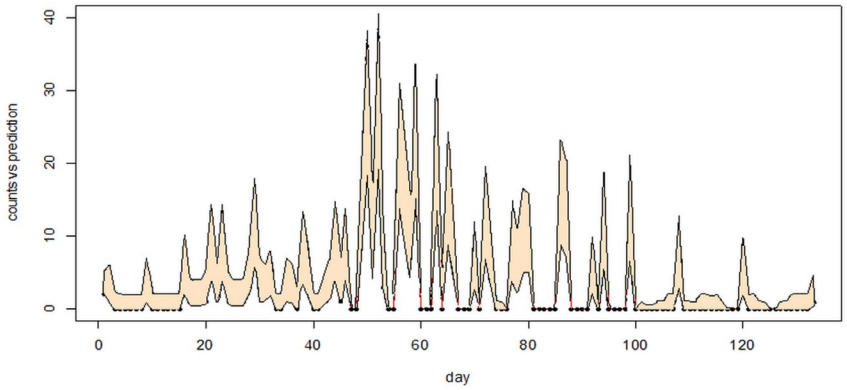

FIGURE 6 Fitted posterior medians versus observed counts of BT disease occurrence (dashed lines represent 95% credible intervals)

In the following figure (Figure 5), we plot the different fitted kernel functions for the three best ZIP models and for a distance between 1 and 60 km. The first two kernel functions, A and B, show short distance dependence, especially the Gaussian kernel B.

Specifically, the Gaussian kernel indicates that the major incidents in the spread of the disease during the epidemic were located in distances approximately up to 12 km, whereas the Exponential kernel suggests a disease spread up to distances of 35 km. On the other hand, the fat-tailed kernel C shows approximately a distance-independent behaviour.

Finally, Figure 6 depicts the observed number of BTV-infected flocks compared to the fitted posterior median number of BTV-infected flocks under the best model (i.e. ZIP model with a Gaussian kernel B) and the corresponding 95% pointwise credible intervals. It is immediately apparent that the fitted and observed incidents are in close agreement, indicating a good fit of the model to our data.

4 | DISCUSSION

During 2014, an epidemic of BTV attributed to serotype 4 occurred in Greece and spread to Bulgaria, Romania, Serbia, Hungary, Albania, Croatia, the Republic of North Macedonia, Montenegro and Turkey (Niedbalski, 2015; World Organisation for Animal Health, 2015). In total, 2,895 outbreaks of BT have been reported by the veterinary authorities of Greece in 2014, reaching 75,412 reported clinical cases of the disease; sheep, goats and cattle were affected with officially reported morbidity rates of 11.0%, 2.0% and 3.5%, respectively (Kyriakis et al., 2015; Vasileiou et al., 2016).

In the current article, we present for the first time the data from the 2014 bluetongue epidemic which occurred between August and December of 2014 in the island of Lesvos, Greece, and utilize them for analyses, especially concerning the spatial and temporal aspects of the epidemic. Specifically, we conducted a spatio-temporal analysis in order to describe the spread of the BT virus between the infected farms and present measures of spatial autocorrelation in order to identify potential spatial patterns in disease transmission.

Considering the spatio-temporal description of the epidemic, the Moran's *I* test in most time periods indicates statistically significant spatial autocorrelations, hence the pattern of the spread of the epidemic in Lesvos seems to be non-random indicating small to moderate positive spatial autocorrelation, which is reinforced by the results of the Geary's *C* coefficients.

The Bayesian regression models suggest that BTV is more likely to spread between closely located farms. BTV is a vector-borne disease, transmitted by *Culicoides* biting midges; therefore, their flying range provides an implicit upper bound to the distance of disease spread (Kluiters, Swales, & Baylis, 2015; Szmaragd et al., 2009). Furthermore, in all the models, the spatial kernel parameter α was statistically significant for the occurrence of the disease, suggesting that there is a positive association between new infections and spatial spread of the disease. Our selected ZIP model is based upon the Gaussian kernel part, which indicates that during the epidemic the majority of the incidents in the spread of BT were located in distances smaller than 12 km. Since our best selected model is based upon the Gaussian kernel part, we have strong evidence to suggest that a circle radius around 12 km at the onset of a similar epidemic in the region could both limit economic damage and prove sufficient in restricting the initial epidemic growth.

Various studies have also attempted to model the spatial distribution of the occurrence of BTV. For instance, Szmaragd et al. (2009) develop a stochastic, spatial farm-level model to describe the spread of BTV within and between farms, using data on the spread of BT virus in Great Britain in 2007 and underlined their analysis by the assumption that the attractiveness of a farm for vector feeding is based on the number of livestock on the farm and is determined by distance to neighbouring farms and the number of livestock. In another study, Ensoy, Aerts, Welby, Stede, and Faes (2013) develop a susceptible-infected spatio-temporal transmission model for capturing the local transmission of between-farm occurrence of the disease, using data on the 2006 BT (BTV-8) epidemic in cattle farms in Belgium. Their study is based on the suggestion that *Culicoides* midges would cause more transmission in shorter distances as compared to longer distances. The neighbourhood assumption based on contiguous regions was deemed appropriate, given the fact that although *Culicoides* midges can be dispersed by the wind to great distances, dispersal over land follow a hopping pattern, that is with

intermediary stops (Hendrickx et al., 2008) and with the midges being able to fly a mean distance of 2 km (Mellor, 1990). Results from the model indicated that temperature, precipitation, farm density, land area and proportion of pasture are important covariates for describing the BT dynamics.

Supporting our suggestion of the 12-km distance between the major incidents in the spread of BT, Hendrickx et al. (2008) showed that 50% of cases occur within 5 km of the previous case, while 95% of cases occurred within 31 km of it. This happens even though BTV is non-contagious since presence of infection in neighbouring municipalities implies that a vector with the virus might be present, can be transported to the neighbouring municipality and may bite the animal in that municipality, causing the transmission of BTV.

We did not consider the effect of meteorological variables in this epidemic. However, it has been observed (see for example Malesios et al., 2016) that their effect is materially negligible in the presence of acute short-lived epidemics, of the kind considered in the present paper. Therefore, the absence of such variables is not expected to have any material bearing upon the conclusions of this work.

In addition, we noted that in the absence of exact spatial allocation of the farm density of the island, we have utilized a random spatial distribution of the farms within each municipality (average surface of municipalities is 124.32 km^2). Our results are, therefore, conditional upon this allocation process. However, each municipality represents a relatively small area and the actual position of the susceptible farms cannot vary substantially. Therefore, the lack of geographic coordinates is not expected to materially affect the results and the fit of the model provides evidence in this direction.

In summary, we investigated the effect of spatial transmission of BTV from infected to non-infected small ruminants' farms in the island of Lesvos, Greece. Spatial analysis showed that disease outbreaks appear clustered due to spatial dependence during the 2014 BTV serotype 4 incursion in Greece. Furthermore, we described the application of spatial Bayesian regression to predict the occurrence of the disease. A zero-inflated Poisson regression model, incorporating serial correlation through an Ornstein–Uhlenbeck process and spatial dependence through a light-tailed kernel part had adequate predictive ability. The simultaneous consideration of the temporal component of disease evolution did not alter the intuitively reasonable conclusion of the absence of long-range transmission for these data. Information derived by our model can be used to anticipate changes in the spatio-temporal distribution of disease and to assist in surveillance efforts. This analysis showed that the epidemic emerged from one location and then transmitted following a non-random (mostly localized) spatial pattern.

ACKNOWLEDGMENTS

The authors would like to thank the 'Directorate of Rural Economy and Veterinary Medicine, regional unit of Lesvos' for the assistance in the data acquisition. N.D. acknowledges support from the Athens University of Economics and Business' Research Centre Action: 'Original Scientific Publications'.

CONFLICT OF INTEREST

The authors declare no conflict of interest.

ETHICAL STATEMENT

The authors declare that ethical statement is not applicable because sample collection or questionnaires from animals has been gathered.

DATA AVAILABILITY STATEMENT

The data that support the findings of this study are available from the corresponding author upon reasonable request.

ORCID

Chrisovalantis Malesios https://orcid.org/0000-0003-0378-3939

REFERENCES

Calistri, P., Giovannini, A., Conte, A., Nannini, D., Santucci, U., Patta, C., … Caporale, V. (2004). Bluetongue in Italy: Part I. *Veterinaria Italiana*, *40*, 243–251.

Caporale, M., Di Gialleonorado, L., Janowicz, A., Wilkie, G., Shaw, A., Savini, G., … Palmarini, M. (2014). Virus and host factors affecting the clinical outcome of bluetongue virus infection. *Journal of Virology*, *88*, 10399–10411. https://doi.org/10.1128/JVI.01641-14

Deardon, R., Brooks, S. P., Grenfell, B. T., Keeling, M. J., Tildesley, M. J., Savill, N. J., … Woolhouse, M. E. J. (2010). Inference for individual-level models of infectious diseases in large populations. *Statistica Sinica*, *20*, 239–261.

Ensoy, C., Aerts, M., Welby, S., Van der Stede, Y., & Faes, C. (2013). A Dynamic spatio-temporal model to investigate the effect of cattle movements on the spread of bluetongue BTV-8 in Belgium. *PLoS ONE*, *8*, e78591. https://doi.org/10.1371/journal.pone.0078591

Federici, V., Goffredo, M., Mancini, G., Quaglia, M., Santilli, A., Di Nicola, F., … Savini, G. (2019). Vector competence of Italian populations of culicoides for some bluetongue virus strains responsible for recent Northern African and European outbreaks. *Viruses*, *11*, 941. https://doi.org/10.3390/v11100941

Geary, R. C. (1954). The contiguity ratio and statistical mapping. *The Incorporated Statistician*, *5*, 115–145. https://doi.org/10.2307/2986645

Greek Ministry of Rural Development and Food (2015). *Πρόγραμμα Επιτήρησης Καταρροϊκού Πυρετού του Προβάτου* (in Greek). Retrieved from http://www.minagric.gr/images/stories/docs/agrotis/poulerika/ya28_3266_140115.pdf

Greek Ministry of Rural Development and Food. (2019, January 3). Ενημέρωση για νέες εστίες Καταρροϊκού Πυρετού έτους 2018 [pdf file]. Retrieved from http://www.minagric.gr/images/stories/docs/agrotis/Aigoprobata/kataroikos_piretos030119.pdf

Hendrickx, G., Gilbert, M., Staubach, C., Elbers, A., Mintiens, K., Gerbier, G., & Ducheyne, E. (2008). A wind density model to quantify the airborne spread of Culicoides species during north-western Europe bluetongue epidemic, 2006. *Preventive Veterinary Medicine*, *87*, 162–181. https://doi.org/10.1016/j.prevetmed.2008.06.009

Kluiters, G., Swales, H., & Baylis, M. (2015). Local dispersal of palaearctic *Culicoides* biting midges estimated by mark-release-recapture. *Parasites & Vectors*, *8*, 86. https://doi.org/10.1186/s13071-015-0658-z

Kyriakis, C. S., Billinis, C., Papadopoulos, E., Vasileiou, N. G., Athanasiou, L. V., & Fthenakis, G. C. (2015). Bluetongue in small ruminants: An opinionated review, with a brief appraisal of the 2014 outbreak of the disease in Greece and the south-east Europe.

Veterinary Microbiology, *181*, 66–74. https://doi.org/10.1016/j.vetmic.2015.08.004

Lessler, J., Salje, H., Grabowski, M. K., & Cummings, D. A. (2016). Measuring spatial dependence for infectious disease epidemiology. *PLoS ONE*, *11*, e0155249. https://doi.org/10.1371/journal.pone.0155249

Li, H., Calder, C. A., & Cressie, N. (2007). Beyond Moran's I: Testing for spatial dependence based on the spatial autoregressive model. *Geographical Analysis*, *39*, 357–375. https://doi.org/10.1111/j.1538-4632.2007.00708.x

Lunn, D. J., Thomas, A., Best, N., & Spiegelhalter, D. (2000). WinBUGS – A Bayesian modelling framework: Concepts, structure, and extensibility. *Statistics and Computing*, *10*, 325–337. https://doi.org/10.1023/A:1008929526011

Malesios, C., Demiris, N., Kalogeropoulos, K., & Ntzoufras, I. (2017). Bayesian epidemic models for spatially aggregated count data. *Statistics in Medicine*, *36*, 3216–3230. https://doi.org/10.1002/sim.7364

Malesios, C., Demiris, N., Kostoulas, P., Dadousis, K., Koutroumanidis, T., & Abas, Z. (2016). Spatio-temporal modeling of foot-and-mouth outbreaks. *Epidemiology and Infection*, *144*, 2485–2493. https://doi.org/10.1017/S095026881600087X

Manso-Ribeiro, J., Rosa-Azevedo, J., Noronha, F., Braco-Forte-Junior, M., Grave-Periera, C., & Vasco-Fernandes, M. (1957). Fievre catarrhale du mouton (blue-tongue). *Bulletin De L'office International Des Epizooties*, *48*, 350–367.

Mayo, C. E., Mullens, B. A., Reisen, W. K., Osborne, C. J., Gibbs, E. P. J., Gardner, I. A., & MacLachlan, N. J. (2014). Seasonal and interseasonal dynamics of bluetongue virus infection of dairy cattle and *Culicoides sonorensis* midges in northern California – Implications for virus overwintering in temperate zones. *PLoS ONE*, *9*, e106975. https://doi.org/10.1371/journal.pone.0106975

Mellor, P. S. (1990). The replication of bluetongue virus in Culicoides vectors. *Current Topics in Microbiology and Immunology*, *162*, 143–161.

Moran, P. A. P. (1950). Notes on continuous stochastic phenomena. *Biometrika*, *37*, 17–23. https://doi.org/10.2307/2332142

Niedbalski, W. (2015). Bluetongue in Europe and the role of wildlife in the epidemiology of disease. *Polish Journal of Veterinary Sciences*, *18*, 455–461. https://doi.org/10.1515/pjvs-2015-0060

Nomikou, K., Mangana-Vougiouka, O., & Panagiotatos, D. E. (2004). Overview of bluetongue in Greece. *Veterinaria Italiana*, *40*, 108–115.

Oravecz, Z., & Tuerlinckx, F. (2011). The linear mixed model and the hierarchical Ornstein-Uhlenbeck model: Some equivalences and differences. *British Journal of Mathematical and Statistical Psychology*, *64*, 134–160. https://doi.org/10.1348/000711010X498621

Purse, B. V., Mellor, P. S., Rogers, D. J., Samuel, A. R., Mertens, P. P., & Baylis, M. (2005). Climate change and the recent emergence of bluetongue in Europe. *Nature Reviews Microbiology*, *3*, 171–181. https://doi.org/10.1038/nrmicro1090

QGIS Development Team. (2015). QGIS geographic information system [website]. Retrieved from http://qgis.osgeo.org

Randolph, S. E., & Rogers, D. J. (2010). The arrival, establishment and spread of exotic diseases: Patterns and predictions. *Nature Reviews Microbiology*, *8*, 361–371. https://doi.org/10.1038/nrmicro2336

Rojas, J. M., Rodríguez-Martín, D., Martín, V., & Sevilla, N. (2019). Diagnosing bluetongue virus in domestic ruminants: Current perspectives. *Veterinary Medicine: Research and Reports*, *10*, 17–27. https://doi.org/10.2147/VMRR.S163804

Scott, P. (2011). *Bluetongue in cattle and sheep [web page]*. Retrieved from https://www.nadis.org.uk/disease-a-z/cattle/bluetongue-in-cattle-and-sheep/

Sokal, R. R., & Oden, N. L. (1978). Spatial autocorrelation in biology: 1. Methodology. *Biological Journal of the Linnean Society*, *10*, 199–228. https://doi.org/10.1111/j.1095-8312.1978.tb00013.x

Spiegelhalter, D. J., Best, N. G., Carlin, B. P., & Van Der Linde, A. (2002). Bayesian measures of model complexity and fit. *Journal of the Royal Statistical Society B*, *64*, 583–639. https://doi.org/10.1111/1467-9868.00353

Stone, M. (1977). An asymptotic equivalence of choice of model by cross-validation and Akaike's criterion. *Journal of the Royal Statistical Society B*, *39*, 44–47. https://doi.org/10.1111/j.2517-6161.1977.tb01603.x

Szmaragd, C., Wilson, A. J., Carpenter, S., Wood, J. L. N., Mellor, P. S., & Gubbins, S. (2009). A modeling framework to describe the transmission of bluetongue virus within and between farms in Great Britain. *PLoS ONE*, *4*, e7741. https://doi.org/10.1371/journal.pone.0007741

Taylor, J. M. G., Cumberland, W. G., & Sy, J. P. (1994). A stochastic model for analysis of longitudinal AIDS data. *Journal of the American Statistical Association*, *89*, 727–736. https://doi.org/10.1080/01621459.1994.10476806

Taylor, W. P. (1986). The epidemiology of Bluetongue. *Revue Scientifique Et Technique*, *5*, 351–356. https://doi.org/10.20506/rst.5.2.256

Vasileiou, N. G. C., Fthenakis, G. C., Amiridis, G. S., Athanasiou, L., Birtsas, P. K., Chatzopoulos, D., … Billinis, C. (2016). Experiences from the 2014 outbreak of bluetongue in Greece. *Small Ruminant Research*, *142*, 61–68. https://doi.org/10.1016/j.smallrumres.2016.02.010

Wilson, A. J., & Mellor, P. S. (2009). Bluetongue in Europe: Past, present and future. *Philosophical Transactions of the Royal Society of London B*, *364*, 2669–2681. https://doi.org/10.1098/rstb.2009.0091

World Organisation for Animal Health. (2013). *BLUETONGUE [pdf file]*. Retrieved from http://www.oie.int/fileadmin/home/eng/animal_health_in_the_world/docs/pdf/disease_cards/bluetongue.pdf

World Organisation for Animal Health. (2015). *World Animal Health Information Database (WAHID) interface [web page]*. Retrieved from http://www.oie.int/wahis_2/public/wahid.php/Diseaseinformation/statusdetail

How to cite this article: Malesios C, Chatzipanagiotou M, Demiris N, et al. A quantitative analysis of the spatial and temporal evolution patterns of the bluetongue virus outbreak in the island of Lesvos, Greece, in 2014. *Transbound Emerg Dis*. 2020;00:1–13. https://doi.org/10.1111/tbed.13553

APPENDIX

TABLE A1 Temporal distribution of confirmed clinical cases of bluetongue in Lesvos, Greece

Day/month/year	Confirmed clinical cases	Total number of animals in infected farms
5–6/8/2014	5	765
13/8/2014	4	439
20–22/8/2014	18	3,097
25–27/8/2014	22	7,042
1–5/9/2014	29	8,238
8–12/9/2014	20	5,306
15–19/9/2014	25	6,545
22–26/9/2014	92	28,016
29–30/9/2014 & 1–2/10/2014	79	42,202
6–9/10/2014	51	5,295
13–16/10/2014	26	8,977
20–23/10/2014	38	7,483
29–30/10/2014	32	5,553
4–6/11/2014	18	3,456
11/11/2014	15	1,921
18–20/11/2014	9	1,833
2/12/2014	6	200
15/12/2014	1	765
Total	490	136,368

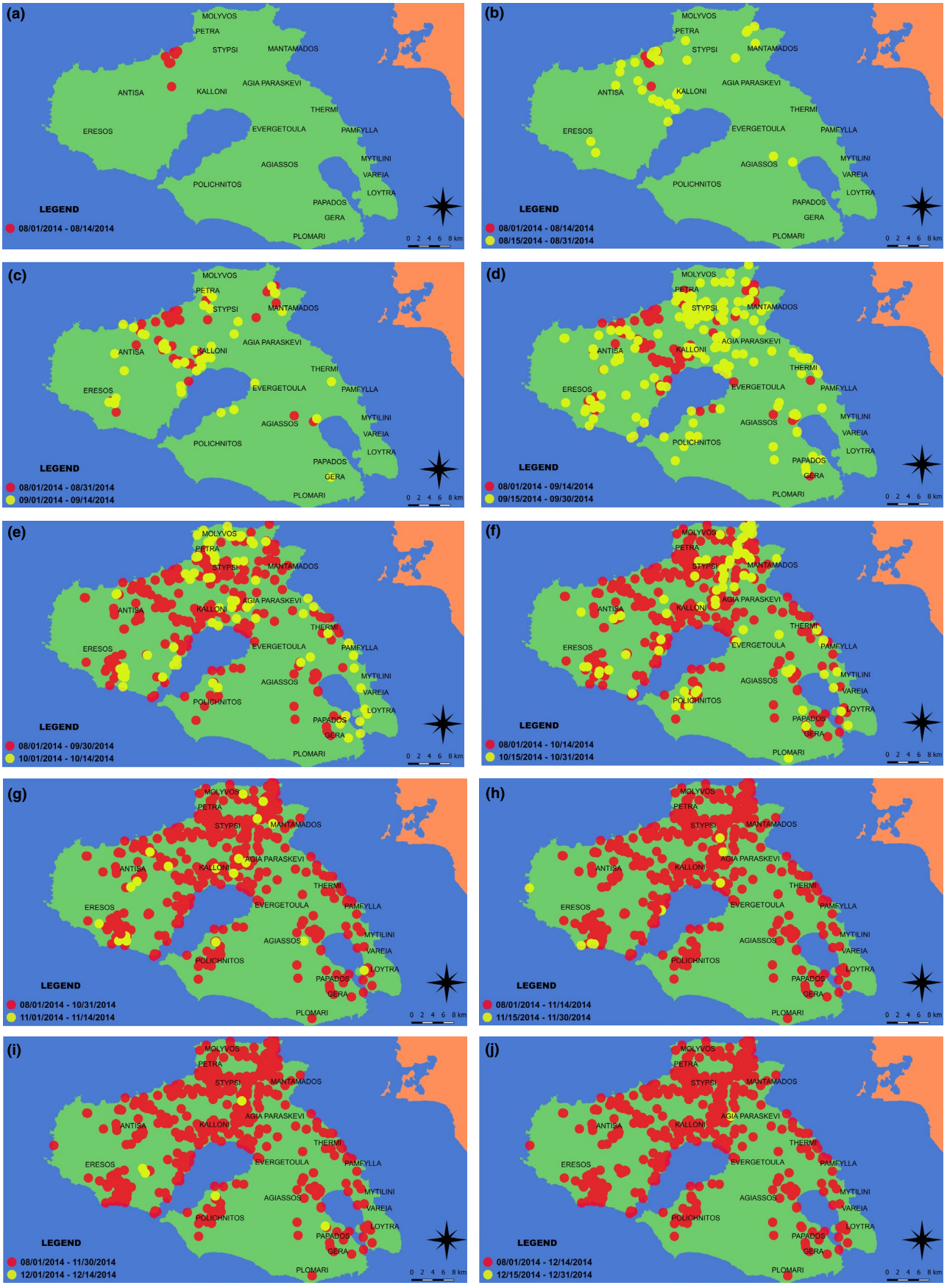

FIGURE A1. Point maps describing the spatial density of BT disease occurrence in the island of Lesvos during the period August–December 2014